Fabrication and Characterization of Superparamagnetic Magnetite (Fe_3O_4) Nanoparticles

Matea Trevino

A senior thesis submitted to the faculty of
Brigham Young University
in partial fulfillment of the requirements for the degree of

Bachelor of Science

Karine Chesnel, Advisor

Department of Physics and Astronomy

Brigham Young University

August 2013

ABSTRACT

Fabrication and Characterization of Superparamagnetic

Magnetite (Fe_3O_4) Nanoparticles

Matea Trevino

Department of Physics and Astronomy

Bachelor of Science

In this thesis, we will discuss the fabrication of magnetite (Fe_3O_4) nanoparticles, their structural characterization through X-ray Diffraction (XRD) and Transmission Electron Microscopy (TEM), and their magnetic characterization through Vibrating Sample Magnetometer (VSM). XRD will give us information about the crystallite quality of the nanoparticles and their average size. TEM will allow us to visualize the nanoparticles, when deposited on a substrate. We will then do bulk magnetization characterization using the VSM. For when they are small enough, magnetite nanoparticles follow a special magnetic behavior called superparamagnetism. This behavior is characterized by a blocking temperature, below which the particles are magnetically frozen. We learn that our nanoparticles show different structural and magnetic properties depending on the preparation method.

ACKNOWLEDGEMENTS

I would like to thank my family for pushing me forward and for trying to help me during this crucial time in my life. I would also like to thank Dr. Roger Harrison and graduate student, Betsy Olsen, for all of their support and help in teaching me chemistry. I would like to thank our graduate student, Yanping Cai, for all of his efforts in helping me finish up my thesis, and hopefully helping in his own thesis. I would also like to thank the people who are reading this thesis right now. I hope that you find what is inside useful towards your own research. Finally, I would like to thank my advisor, Dr. Karine Chesnel, for her understanding and help towards this thesis during a crucial and critical time in her life. I fully appreciate what you have done for me and I hope that this thesis will be useful for the future studies that will be carried out in your group.

Table of Contents

List of Figures

Chapter 1

INTRODUCTION

1.1 Scientific Context

Our generation is all about smaller is better. We need to get the smallest phone, tools, and computers and they need to have the latest technology in them and be able to do everything that we need them to do. Medicine is also turning this way. People in the medical engineering field are trying to think of the smallest tools that they can use in order to have the most efficient treatments. They are thinking of using different types of materials that will have the job of carrying medicine to a specific place in the body. There it will release a concentrated dosage of medication to only that specific place; magnetite (Fe_3O_4) nanoparticles are one of these options [1]. In order to do this, we need to understand the behavior of such nanoparticles. The purpose of this thesis is to investigate different fabrications of magnetite nanoparticles, and the superparamagnetic behavior of magnetite nanoparticles, using different techniques. I will first generally explain superparamagnetic behavior and past research on magnetite nanoparticles. I will then discuss our fabrication methods and results of our bulk magnetization characterization. Finally, I will discuss the importance of my results and provide suggestions for future research.

1.2 Superparamagnetic Behavior

Magnetite (Fe_3O_4) nanoparticles have a special behavior called superparamagnetism. In each nanoparticle, there are thousands of Fe atoms, and each atom carries an individual spin. Within each particle, all the Fe spins are strongly interacting, and aligning in the same direction, thus forming a macrospin. The question now is how the macrospins carried by each nanoparticle interacts between each other at the nanoscale. It is found in our magnetite nanoparticle assemblies that the macrospins exhibit a superparamagnetic behavior. To understand what superparamagnetism means, we should first explain what paramagnetism is. When a material exhibits a paramagnetic behavior, its net magnetization is zero in the absence of an external field. This is due to the fact that the individual spins, or magnetic moments, are randomly aligned to equal a net magnetization of zero. When an external field is applied, a net magnetic moment appears in the direction of the applied field. This is like having a set of pool balls being our magnetic system, where each ball corresponds to a single spin; it has a number on one side which will indicate the direction of the field. We then put down the pool triangle and fill it full of the pool balls. Notice that you can move them around and that the number goes wherever it wants to go. If we continued to move the balls around and then let them rest the way they landed, that would most likely be when there is no field applied to the system, being the pool triangle. If we had all the numbers of the pool balls facing up or facing down that means there is a field applied to the object, either in a positive direction, up, or a negative direction, down. Now let's say that each pool ball is one nanoparticle, instead of an atom, and we keep the same set up, in that the balls are in the pool triangle and they are set up in a random formation. The same rules apply; the only difference is the size. This difference in size is how we describe superparamagnetic behavior; it means

that we are looking at a paramagnetic behavior in terms of macrospins, where one nanoparticle is a macrospin, instead of atomic spins. The assembly of nanoparticles as a system has a paramagnetic behavior; so that means that it still is neutral when there is no field applied but when a field is applied to the sample, then the macrospins will align with the field.

With the nanoparticles being superparamagnetic, this means that they also exhibit certain characteristics. One of these characteristics is that nanoparticles exhibit a blocking temperature at low temperatures [2]. The blocking temperature is when the system undergoes a phase transition and becomes magnetically "frozen." This can be explained with our pool ball analogy. We have our balls in the triangle and we can easily move the triangle around, making it easy for all of the balls to move around. Let's then turn the temperature down so low that the triangle is now frozen to the pool table, while the balls are oriented with the magnetic field. When this happens that is the blocking temperature. This is what we are focusing our research on the magnetic characterization of different of magnetite nanoparticles, made by an inorganic salt method, an inorganic solution method, or an organic solution method. I will also discuss why this is important to us and what potential it could hold for technology in the next section.

1.3 Literature Review

The superparamagnetic properties of the magnetite nanoparticles have been investigated by several groups. For example, Krycka et al. looked at the internal structure of the nanoparticles at a low temperature [3]. They determined that the nanoparticles interact magnetically with each other, meaning that the direction of the magnetic moment (or field of the particle) depends on the magnetic moments of the particles around it. The particles also behave differently when they are in a controlled structure, as in they were grown into a structure and are not in their natural shape. Changes in their shape will cause the structure of the magnetic moments to change to fit with their natural ways. Krycka et al. also wrote a letter about the magnetic morphology of structurally uniformed nanoparticles [4]. They have measured that their nanoparticles are round in shape. This means that the shape and the magnetic morphology, distribution of the magnetic field, of the nanoparticles are isotropic. Other scientists have mentioned that the size of the nanoparticles will affect the blocking temperature of the nanoparticles [5]. They have determined that the smaller the particle, the lower the blocking temperature.

Magnetite nanoparticles are important because of the potential medical usage of the nanoparticles. Peter Majewski and Benjamin Thierry, and Jing et al. have talked about how magnetite nanoparticles can be used for magnetic hyperthermia in order to kill cancer through heat sensitivity [1, 6]. Nunes et al. goes into more details as to how this is more beneficial for medical reasons, due to the fact that magnetite is not harmful to our bodies [7]. They can use this to transfer drugs or to clear out toxic waste from our bodies. They are able to consider this possibility through the unique behavior of the magnetite nanoparticles. Our

job is to better understand the structural and magnetic behavior of magnetite nanoparticles so that we can control them better.

Chapter 2

Fabrication Methods

We have investigated three different approaches to prepare samples. First, an inorganic salt method, second an inorganic solution method, and thirdly an organic solution method. We will see that these three methods lead to different particle sizes.

2.1 Inorganic Salt Method

The process for making magnetite nanoparticles includes the chemical preparation of the Fe_3O_4 compound, which consist in one Fe^{2+} ion with two Fe^{3+} ions [8]:

$$Fe^{2+} + 2Fe^{3+} \rightarrow Fe_3O_4 \ . \tag{2.1}$$

In our preparation, we are not necessarily mixing salts in a stoichiometric ratio, but we adjusted the ratio to obtain the best results according to X-ray Diffraction, as seen in table 1.

We start the inorganic salt method by mixing $FeCl_3$ hydrated salt, $FeCl_2$ hydrated salt, and ammonium bicarbonate (ABC) with distilled water, as seen in figure 1A and 1B.The ratio of the different reactants were varied to explore the effects of starting material ratios on the magnetite purity according to XRD. If we were using the correct ratio, we mixed 16.22 g of $FeCl_3$ hydrated salt, 19.88 g of $FeCl_2$ hydrated salt, and 88.43 g of ABC. If we were using an incorrect ratio, we mixed 19.00 g of $FeCl_3$ hydrated salt, 19.88 g of $FeCl_2$ hydrated salt,

and 92 g of ABC. The iron chlorides and ABC were mixed together with 50 mL of distilled water to make a precursor material with a gaseous byproduct, which looks like brownie mix after 30 minutes of stirring, as can be seen in figure 1C through 1E. We let this paste dry in a drying oven over night at 100 °C, or 12-24 hours, as seen in figure 1F, and rinsed extensively with nitric acid, a strong acid, or distilled water using a vacuum filtration system to remove ammonium chloride. The precursor was then calcined at 550 °C for three and a half hours in a vacuum oven, as seen in figure 1I and 1J. The final product was a black, magnetic powder, seen in figure 1K.

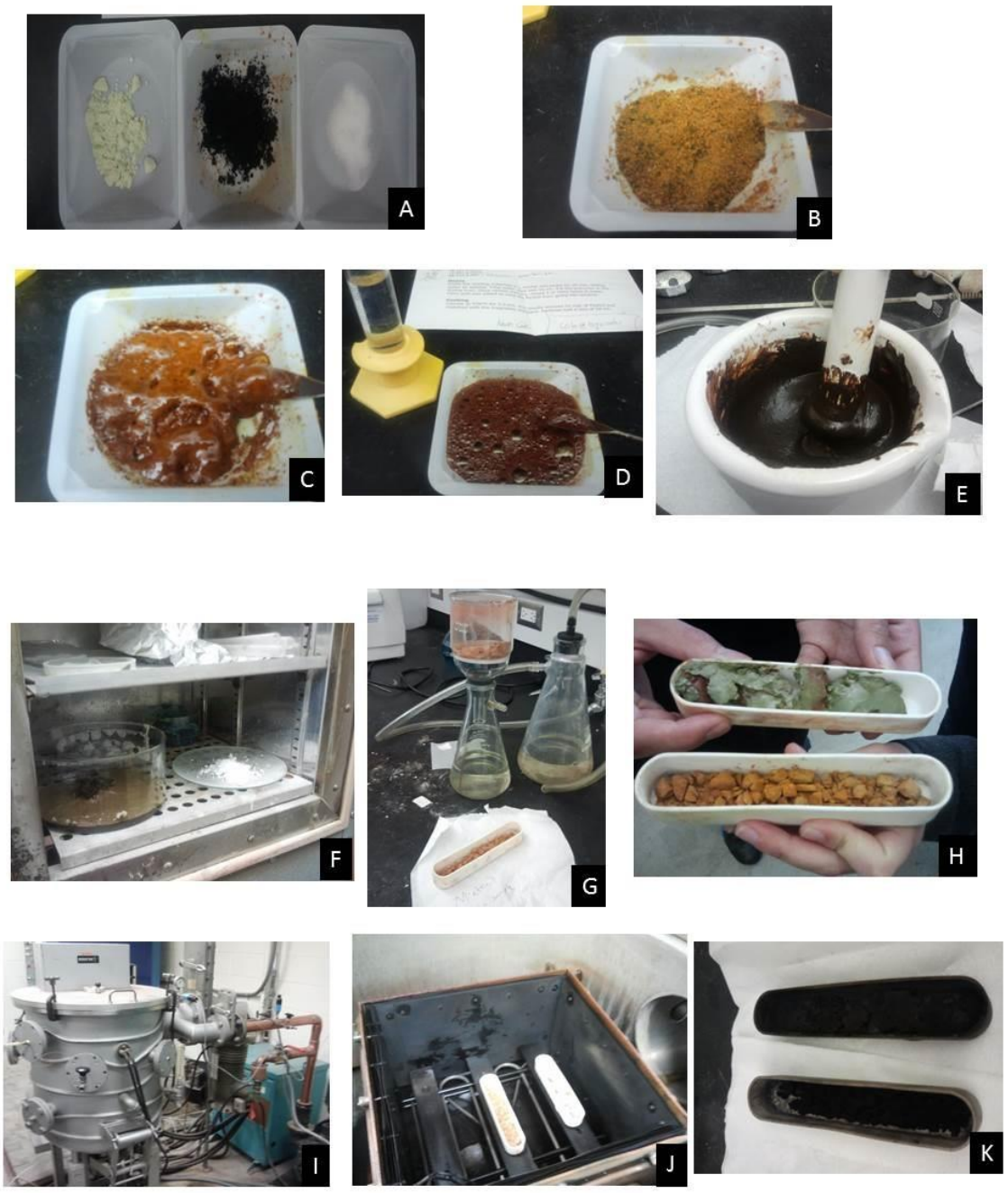

Figure 1 (1A) Reactants in a powder form of the substances $FeCl_2$ hydrated salt, $FeCl_3$ hydrated salt, and ABC respectively, (1B) Mixture of the 3 powders, (1C) Slowly adding and mixing water to the mixture, (1D) Mixture with all the water added to the mixture, (1E) Once mixed the mixture turns into a black paste and is the precursor, (1F) Mixture in a drying oven, (1G 1H) Mixture rinsed with nitric acid or water and put into a ceramic, green is still wet and red is dry (1I 1J) Vacuum oven and the samples in the oven to be baked, (1K) the final product of magnetite

2.2 Inorganic Solution Method

The inorganic solution method consists in mixing two separate solutions [9]. The first solution is a mixture of $FeCl_3$ hydrated (33.238 g) and distilled water (250 mL). The second solution is a mixture of $FeCl_2$ hydrated (24.215 g) and distilled water (250 mL) in a separate volumetric flask, as can be seen in figure 2A. We filter both of the liquids separately, using a vacuum filtration system and discard the solids. The filtered solutions were then combined in a 1.75 ($FeCl_3$) to 1 ($FeCl_2$) ratio. Ammonium hydroxide was then added to the mixture, while stirring, until a pH of 10 was reached, at which point magnetite was precipitated. The mixture was treated twice with approximately 200 mL of boiling distilled water and dried on a vacuum filtration system, as seen in figure 2B. The residue contains magnetite nanoparticles.

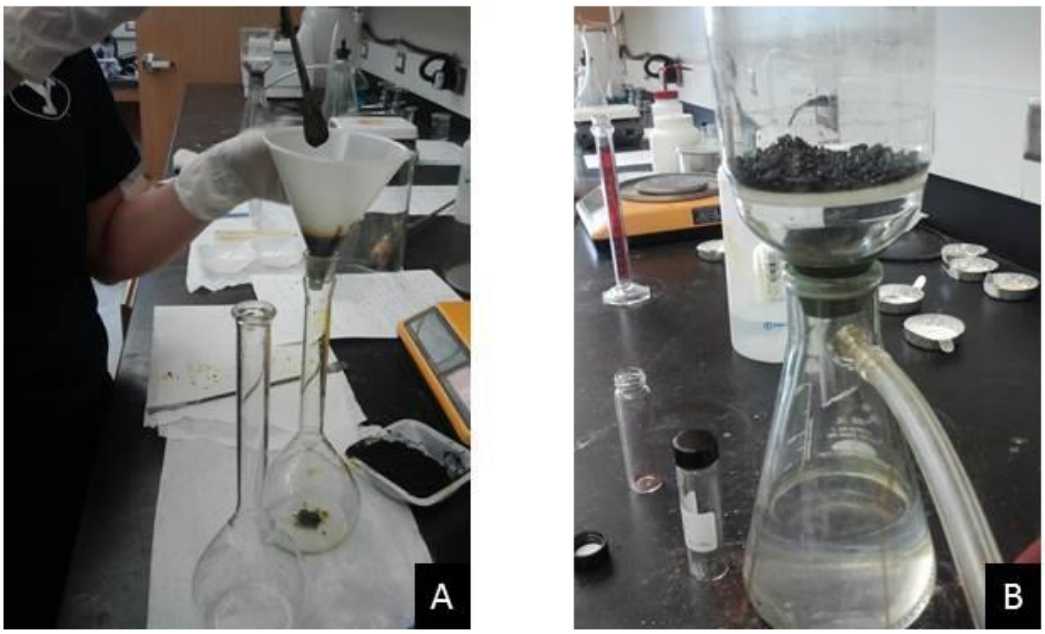

Figure 2 (2A) Mix $FeCl_3$ with water then mix $FeCl_2$ with water, separately mix two solutions together 1.75 ($FeCl_3$) to 1 ($FeCl_2$) treat with boiling water and rinse with 2 L of distilled water, (2B) Dry completely

Sample Name	Type of Method	Ratio of Fe^{2+} to Fe^{3+} in the salt	Rinsed	Specifics
NP01	Inorganic Salt	1.6	Water	
NP02	Inorganic Solution	0.59	Water	Dried for several days at 40 ° C
NP03	Inorganic Solution	0.59	Water	Dried on filter till dry
NP04	Inorganic Solution	0.59	Water	Dried in air at 40 ° C until dry rinsed with 2 L of water then dried on filter
NP05	Inorganic Salt	1.56	Nitric Acid	
NP06	Inorganic Salt	1.33	Nitric Acid	
NP07	Inorganic Solution	0.59	Water	
NP10	Inorganic Salt	1.56	Water	
NP11	Inorganic Salt	1.56	Water	
NP12A	Inorganic Salt	1.33	None	
NP12B	Inorganic Salt	1.33	Water	
NP13A	Inorganic Solution	1.75	None	
NP13B	Inorganic Solution	1.75	Water	

Table 1 Summary of all Inorganic Samples and the preparation used for each

2.3 Organic Solution Method

We investigated an organic solution method to see if it would give us better control of the size of the particles and would let us form a monolayer of the particles. We investigated four different variations of the organic method, as seen in table 2 with the compilation of all of the samples and the method that was used to fabricate them.

In the first method, we follow the preparation described by Altavilla, which is illustrated in figure 3A [10]. We mixed 1.401 g of Fe(III) acetylacetonate with 5.16 g of hexadecane, 40 mL of phenylether, 3.8 mL of oleic acid, and 5.6 mL of olelamine. We then stirred this together and set it on a heating plate, as seen in figure 3B. We heated the solution up to 200 °C for thirty minutes under nitrogen, as seen in figure 3C. We then refluxed the solution, in which we increase the temperature; the temperature was around 250 °C for another thirty minutes. We let the particles cool. Once the particles were at room temperature, we rinse them with 250 mL of ethanol and centrifuge them for three to four minutes, as seen in figure 3D. The centrifuge spins the particles and makes it so that we can separate the nanoparticles from the ethanol. We then decanted off the ethanol and extracted the left over nanoparticles, which were in the form of a black paste that we later dried to a more powder like substance.

Figure 3 (3A) Mixture Fe(III) acetylacetonate with hexadecane, phenylether, oleic acid, and olelamine, (3B) Stir and heat up to 200 °C under nitrogen for thirty minutes, (1C) Refluxes and stays around 250°C for thirty minutes, (1D) Cool down and add ethanol put in centrifuge and decanter off liquid

The second method was inspired from two references, one from Jana et al. and the other from Park et al [11, 12]. The first part of the procedure was done by following Jana et al., which produced an iron oleate, which can be seen in figure 4C [11]. To make the iron oleate, we start by dissolving 5.41 g of $FeCl_3*6H_2O$ in 100 mL of methanol. We then added 17 mL of oleic acid. In a separate flask, we dissolved 2.4 g of NaOH in 200 mL of methanol. We combined this solution with the first solution a few drops at a time, and mixed them together. We filter the solution with a vacuum filter, as seen in figure 4A, and kept the left over liquid, as seen in figure 4B. It was then left to dry overnight under a vacuum, as seen in figure 4C. We then turn to Park et al.'s work to finish synthesizing the nanoparticles [12]. We mix 0.55 g of the previously prepared iron oleate with 0.16 g of oleic acid and 4 g of 1-octadecene. We put the mixture on a heating mantel and heat it up a little to let it dissolve, similar to the setup seen in figure 3B. The solution was heated up to 322 °C and heated for thirty minutes. The solution is then left to cool down to room temperature and 10 mL of ethanol was added to the solution. The solution is then put into the centrifuge and the excess liquid is cantered off, similar to figure 3D. The result is a black paste that we then leave to dry to a more powdery substance.

Figure 4 Mix $FeCl_3*6H_2O$ with methanol and oleic acid joined by a mixture of NaOH and methanol, (3A) Mixture in vacuum filter, (3B) Keep leftover liquid, (3C) Dry under vacuum overnight resulting in iron oleate

The third method is similar to the first method except that we used 1-octadecene instead of phenylether, and for the fourth method phenylether was replaced with trioctylamine. We did this so that we could get a higher reflux temperature. If we achieved a higher reflux temperature then we would potentially get larger nanoparticles.

Sample Name	Type of Method	Specifics	Reflux Temperature
NP09	Organic Solution	First Method	252 °C
NP09W	Organic Solution	First Method Rinsed	252 °C
NP14	Organic Solution	First Method	252 °C
NP15	Organic Solution	Second Method	322 °C
NP16	Organic Solution	Second Method	320 °C
NP17	Organic Solution	Third Method	290 °C
NP18	Organic Solution	First Method	260 °C
NP19	Organic Solution	Fourth Method	310 °C

Table 2 Summary of all Organic method samples with the details of preparation

Chapter 3

Structural Characterization

3.1 X-ray Diffraction

X-ray Diffraction (XRD) is a technique that provides information on the crystallography of the samples; we expect to see an inverse spinel structure for magnetite. We use this technique to determine the structure of the sample and the size of the individual crystallites. This gives us information about the crystallite quality of our magnetite nanoparticles and the size of the particles.

A typical XRD measurement is performed by doing a (θ, 2θ) scan, in which θ is the angle between the incident ray and the sample and 2θ is the angle between the incident ray and the diffracted ray, as seen in figure 5. We use a PANalytical X'Pert instrument to perform the XRD measurements; a picture of the instrument is shown in figure 5A. The x-ray beam comes through the left arm and illuminates the sample. The diffracted x-rays are picked up by the detecting right arm and the detector reads the intensity of the x-rays as a function of angle. In this case the sample stage and the detector arm move simultaneously to keep the (θ, 2θ) geometry, as shown in figure 5B. A graph of intensity vs. 2θ is recorded, as seen in figure 6. When looking at the graph, we can see that there are peaks at certain 2θ angles, where a constructive interference occurs. Each spectrum corresponds to a particular crystallographic structure. We compare our experimental spectrum to templates in order to help us distinguish if we have made magnetite or, it's cousin, hematite (Fe_2O_3), as seen in figure 6. The graph also helps us to determine the size of the crystallites in the sample. This

is done by measuring the width of the peaks. If we had an infinite crystal, the XRD scan would show Dirac peaks, but since we have a powder, made of small nanoparticles, the peaks in the XRD spectrum have width to them. We can estimate the average size of the crystals using the Scherrer equation:

$$d = \frac{K\lambda}{Bcos(\theta)} \tag{3.1}$$

In this equation, θ is the angle that is associated with the position of the peak, and can be found on the x-axis; B is the width of the peak at half max; λ is equal to the wavelength of the x-rays used, in our case λ is equal to 0.15418nm; k is a constant equal to:

$$2\left(\ln\left(\frac{2}{\pi}\right)\right) = 0.9; \tag{3.2}$$

and d is the resulting average diameter of the crystal, which is the diameter of the particles in nm.

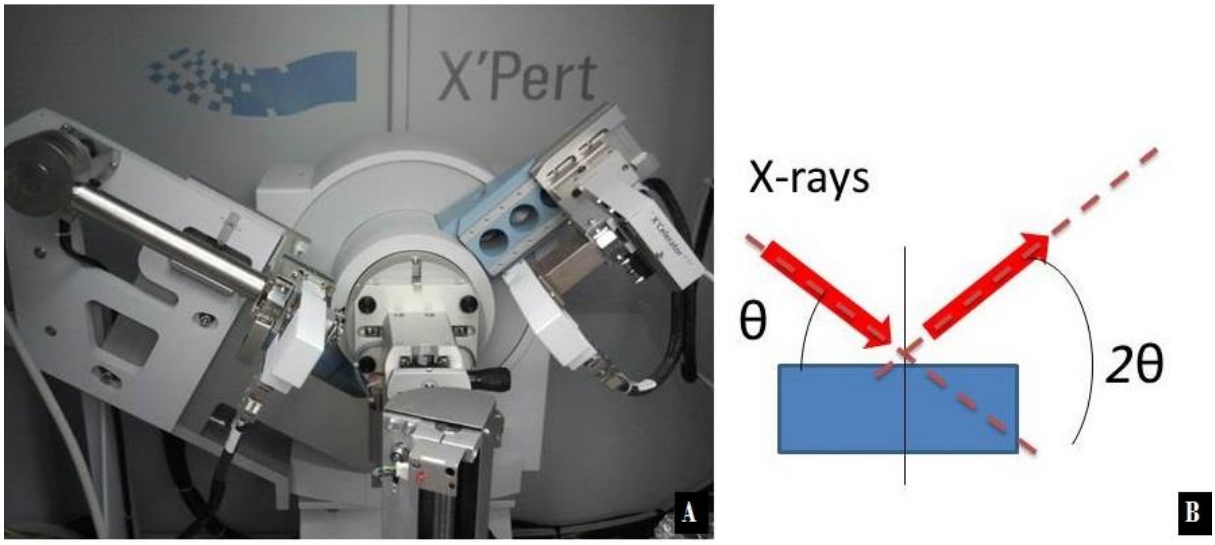

Figure 5 (A)XRD instrument used, x-rays come out of the stationary left arm and illuminate the sample, the moving right arm picks up the scattered x-rays and puts them in a θ to 2θ configuration, (B) Sketch of the (θ, 2θ) scan setup

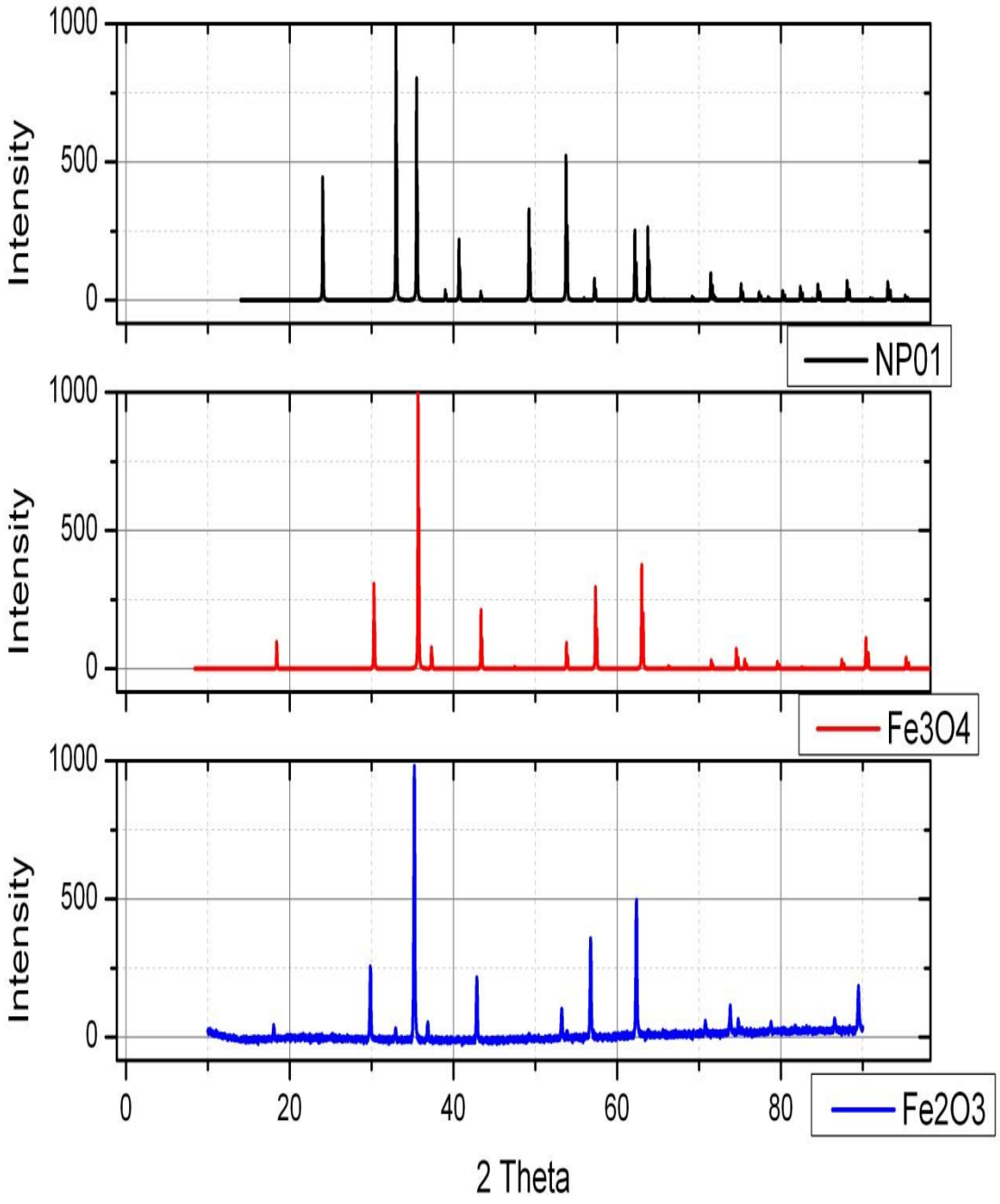

Figure 6 (θ, 2θ) scans of sample NP01, along with standard spectra for Fe_2O_3 and Fe_3O_4

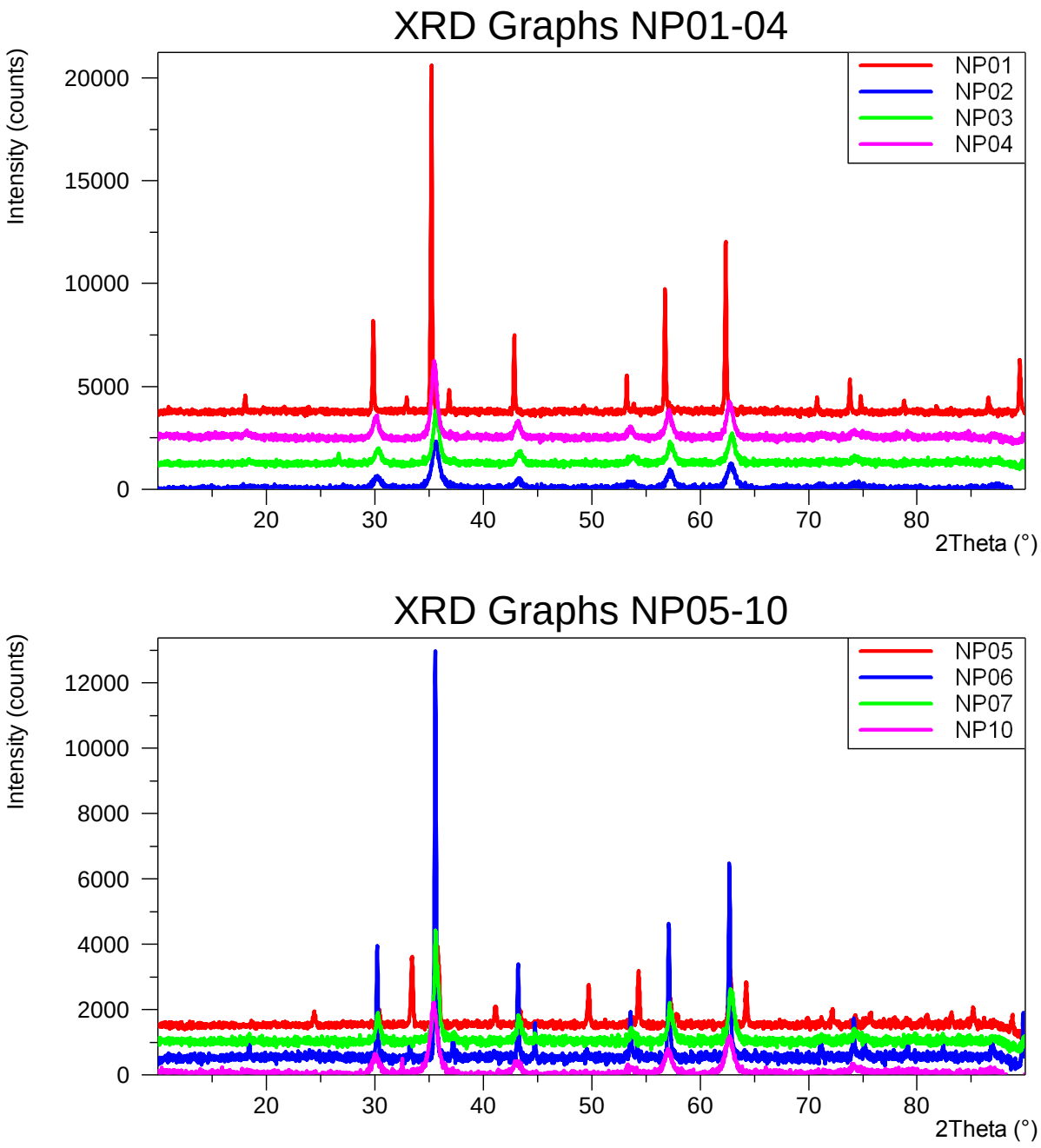

Figure 7 XRD Graphs for samples NP01-10

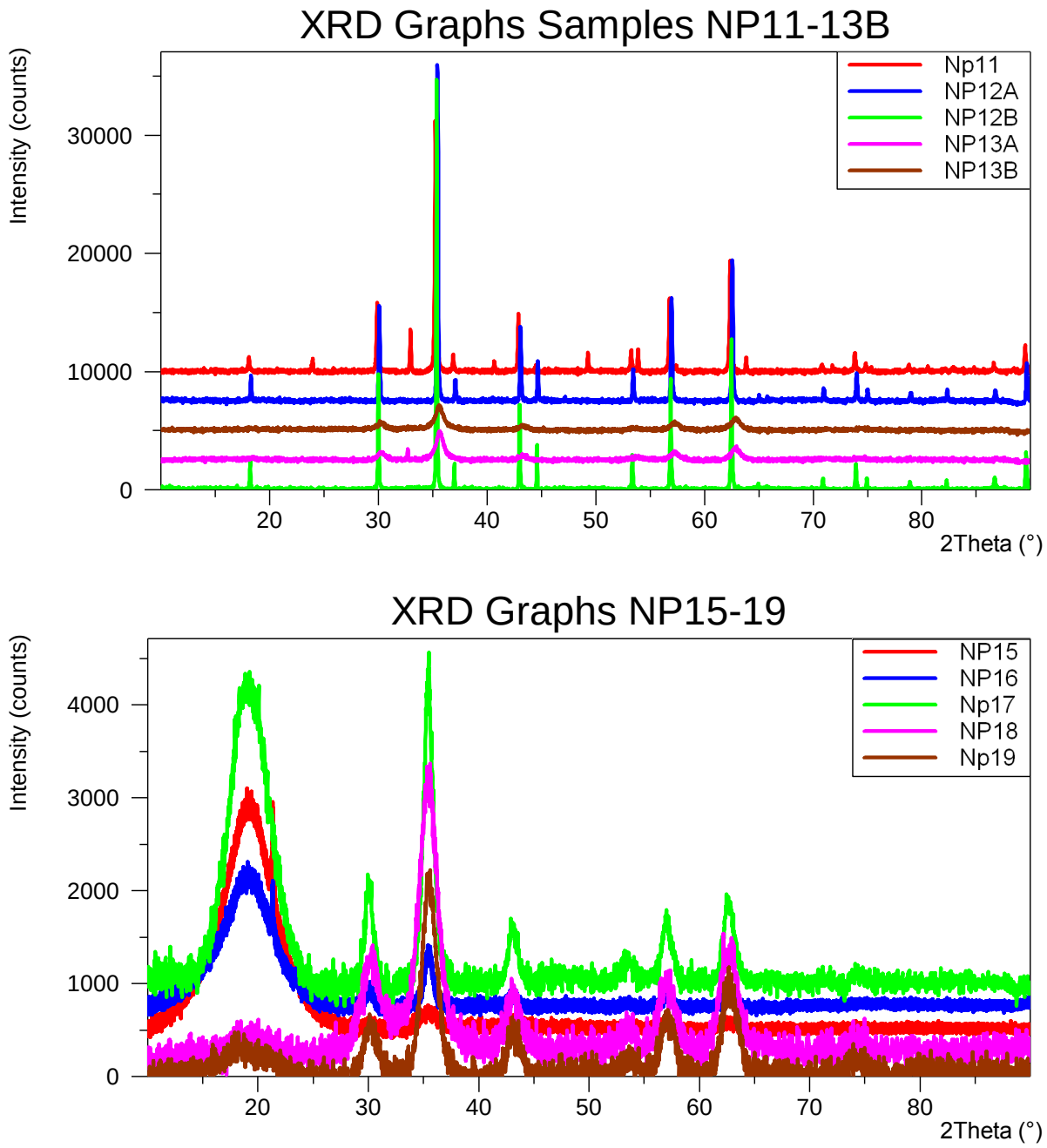

Figure 8 XRD measurements for samples NP11-19

For each sample, the experimental graph is compared to the templates of hematite (Fe_2O_3) and magnetite (Fe_3O_4) to determine if they are considered to be pure magnetite particles or if they contain some hematite. A matching score is found by the X'Pert program. It looks at the peaks and lines them up with the templates that it has in its library. It then determines which compound fits best with the sample and gives it a score based on the peaks placement and intensity, as seen in table 3.

We also had the opportunity to analyze some of our XRD data with a Rietveld refinement. What the Rietveld refinement does is to look at the spectrum and makes a simulation structure of magnetite and can tell us the precise amount of magnetite and hematite that we have in each sample, as seen in figure 9.

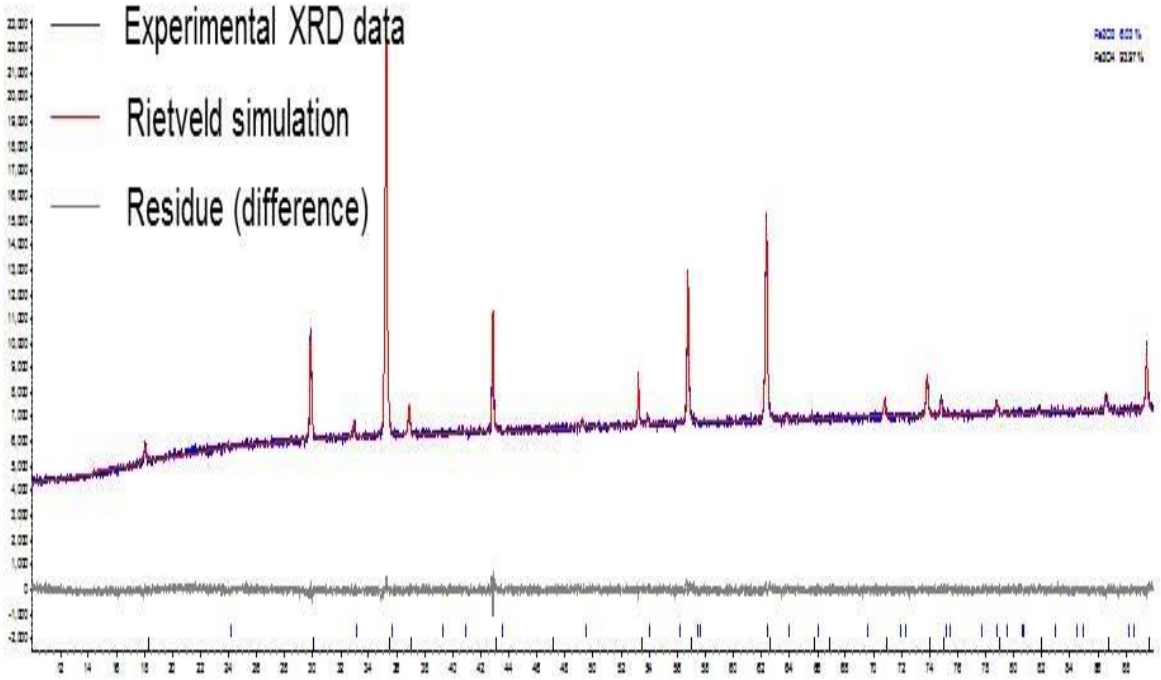

Figure 9 Comparison of XRD Data with Rietveld simulation and the Residue of subtracting the two

Table 3 gives a list of the data found for all of the samples, including the matching score with magnetite, the Rietveld refinement percentage of magnetite for the samples that have been analyzed, and the average size of the particles found through the Scherrer formula.

Sample Name	Fabrication Method	Score for Magnetite	Rietveld Refinement Percentage of Magnetite	Average Size (nm) Scherrer formula
NP01	Inorganic Salt	66	94%	51.9 ± 9.1
NP02	Inorganic Solution	83		9.8 ± 2.5
NP03	Inorganic Solution	40	100%	13.0 ± 5.3
NP04	Inorganic Solution	87	100%	12.2 ± 0.8
NP05	Inorganic Salt	26	34%	35.2 ± 9.1
NP06	Inorganic Slat	71		41.1 ± 5.8
NP07	Inorganic Solution	79		18.7 ± 8.8
NP10	Inorganic Salt	92		10.8 ± 3.9
NP11	Inorganic Salt	38		62.8 ± 11.6
NP12A	Inorganic Salt	89		52.2 ± 7.8
NP12B	Inorganic Salt	85		64.6 ± 15.8
NP13A	Inorganic Solution	80		10.9 ± 2.9
NP13B	Inorganic Solution	86		9.8 ± 1.9
NP14	Organic Solution	87		4.0 ± 0.7
NP15	Organic Solution	90		5.8 ± 1.7
NP16	Organic Solution	94		11.0 ±4.6
NP17	Organic Solution	95		8.5 ± 2.9
NP18	Organic Solution	90		5.5 ± 0.7
NP19	Organic Solution	92		6.4 ± 1.9

Table 3 List of samples with their matching score for matching magnetite template, their calculated percentage of magnetite through Rietveld refinement, and the average size of the particles with the standard deviation of the size

The table indicates our samples match the structure of Fe_3O_4, with a matching score ranging between 26 and 95. This variety of scans is due to the fact that the data is noisy or there are impurities in the sample. We have been able to get more accurate data through the Rietveld refinement and have been able to tell the real percentage Fe_3O_4 and Fe_2O_3 in our samples.

3.2 Transmission Electron Microscopy

The Transmission Electron Microscopy (TEM) is another tool to help us determine the size and the spread of the size of the nanoparticles. The TEM functions by emitting electrons that hit the sample in transmission. The electrons then interact with the sample and the contrast in absorption gives an image of the sample. The sample can then be imaged. The TEM image will then let us know the range of the particles and how the particles align themselves, when they are dropped onto a substrate, as seen in figure 10. We looked at these images and measured the sizes of the individual nanoparticles, from which we calculated a statistical average. This study is described in greater detail in Yanping Cai's master thesis. In table 4, we compare these results with what we have found with the XRD.

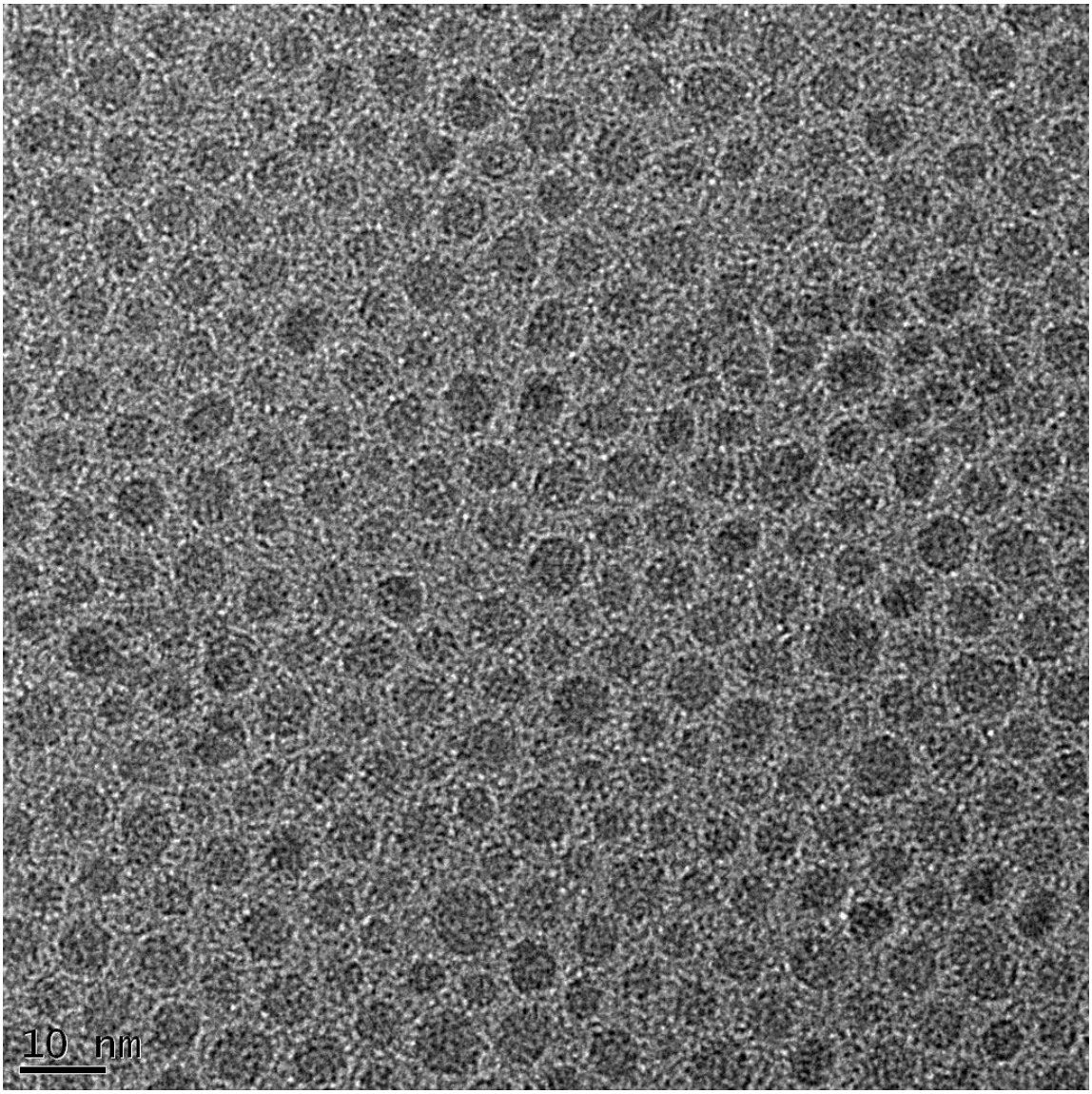

Figure 10 TEM image of NP18, Can see individual nanoparticles, how they self-assemble, and the size of the nanoparticle

Sample Name	Fabrication Method	Average Size (nm) Scherrer formula	Average Size (nm) TEM Images
NP15	Organic Solution	5.8 ± 1.7	6.2 ± 1.0
NP16	Organic Solution	11.0 ±4.6	10.2 ± 2.8
NP17	Organic Solution	8.5 ± 2.9	7.4 ± 1.9
NP18	Organic Solution	5.5 ± 0.7	5.6 ± 1.0

Table 4 Comparison of the average size of the nanoparticles from the XRD and the TEM

The TEM is more accurate than the XRD, when it comes to finding the size of the particles. This is because we can see the actual particles themselves and measure them, with the TEM, and because we have a lot of particles (hundreds) in one given image, so it gives a good statistical overview of them. TEM gives a real space overview of the sample as a whole, whereas the XRD gives an indirect view in the diffraction space, and the quality of the XRD scan depends on the amount of sample and the amount of noise, which could possibly be hiding peaks. Also we have only a few peaks to determine the average size. We find a good agreement between the two techniques confirming the physical results. The average size of the inorganic salt method ranges from 10-64.6 nm in size. The average size of the inorganic solution ranges from 9.8-18.7 nm, and the organic solution ranges from 4.0-11.0 nm in size. The largest particles are the inorganic salt and are not very controllable in size. The inorganic solution produces particles that are a bit more controllable in size. The most controllable size is obtained through the organic solution method.

Chapter 4

Magnetic Characterization

4.1 Vibrating Sample Magnetometry

The vibrating sample magnetometer, or VSM, is an instrument that measures the net magnetization of the nanoparticles. The VSM includes a superconducting magnet that can go up to 9 Tesla (T). In comparison, a refrigerator magnet usually produces a magnetic field of about 0.005T, or 50 Oe. The VSM makes the sample vibrate, to create a magnetic flux (Φ), in a detection coil. The instrument uses the change of magnetic flux in time, and the resulting electromagnetic voltage in the detecting coil, to measure the magnetic moment of the sample. This is based on Faraday's law that states that the change in flux over time equals the negative electromagnetic voltage, or

$$\frac{d\Phi}{dt} = -V_{em}. \tag{4.1}$$

The VSM is used to do magnetization loops, field cooling (FC), and zero field cooling (ZFC) measurements.

4.2 Magnetization Loops

To perform a magnetization loop, we work at a fixed temperature and we sweep the magnetic field, produced by the superconducting magnet, in such a way to cover a wide range of field values on the positive to negative sides and close the loop. We usually start at zero field then go up to the desired field on the positive side, for example +1 T (or 10,000 Oe), and then go down to the same value on the negative side, which would be -1 T, and then back up to zero. The magnetic moment is then plotted as a function of the applied magnetic field, as seen in figure 11. We use the magnetization loops to measure various properties; the shape of the curve indicates the type of magnetic behavior. An 'S' shape generally indicates a ferromagnetic or ferrimagnetic behavior. We do observe an S shape with our magnetite nanoparticles; that are actually ferrimagnetic. From the loop, we can measure the magnetization at saturation (M_S), which is the highest magnetic value the sample can reach at the given temperature. We have also studied if there is a hysteresis, where the ascending and descending branch of the loop are not the same. We do observe a very small hysteresis in our nanoparticles. The hysteresis becomes insignificant when the particles are small enough. We have also studied if the loop changes when the temperature changes. Occasionally, we use magnetization loop measurements to make sure that our sample has stayed in the same position, before and after a cooling procedure. It is indeed very important to make sure that the sample is well aligned at the center of the detection coil. If the sample is not well centered, we could lose a significant amount of signal. Figure 11 shows a series of magnetization loops, recorded on the same sample, placed at different positions z on the holder. We can see that when the sample position deviates from the center of the coil, we

lose the magnetic signal and could possibly observe a flipping of the graph. Therefore, we need to be careful with the placement of our sample.

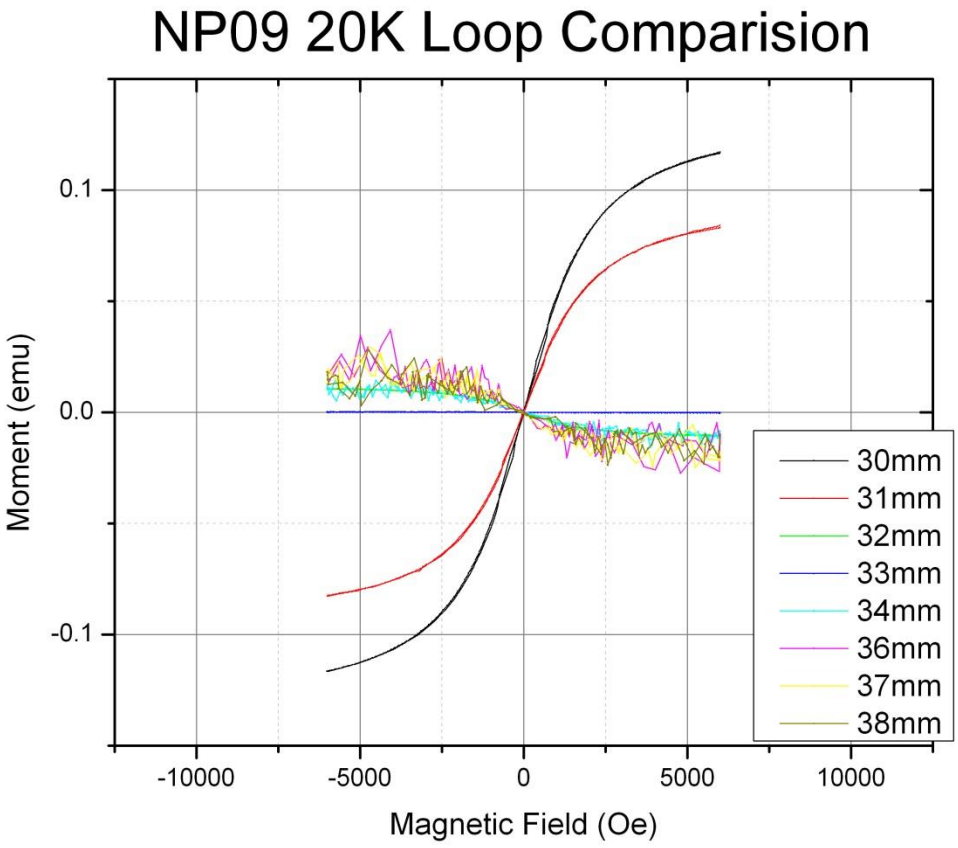

Figure 11 Field loops done at 20K in which the position of the sample was moved

We have measured the saturation point for the different samples. We measure the magnetization at saturation M_S by using the asymptotic line at the positive end of the S shape. We estimate the saturation field H_S by finding the corresponding point on the x-axis. At the saturation point, all of the particles are aligned with the magnetic field. In our case, we find that the saturation is a very soft and slow process, so there is not a precise value for H_S but more like a region of field values, where the particles are mostly aligned.

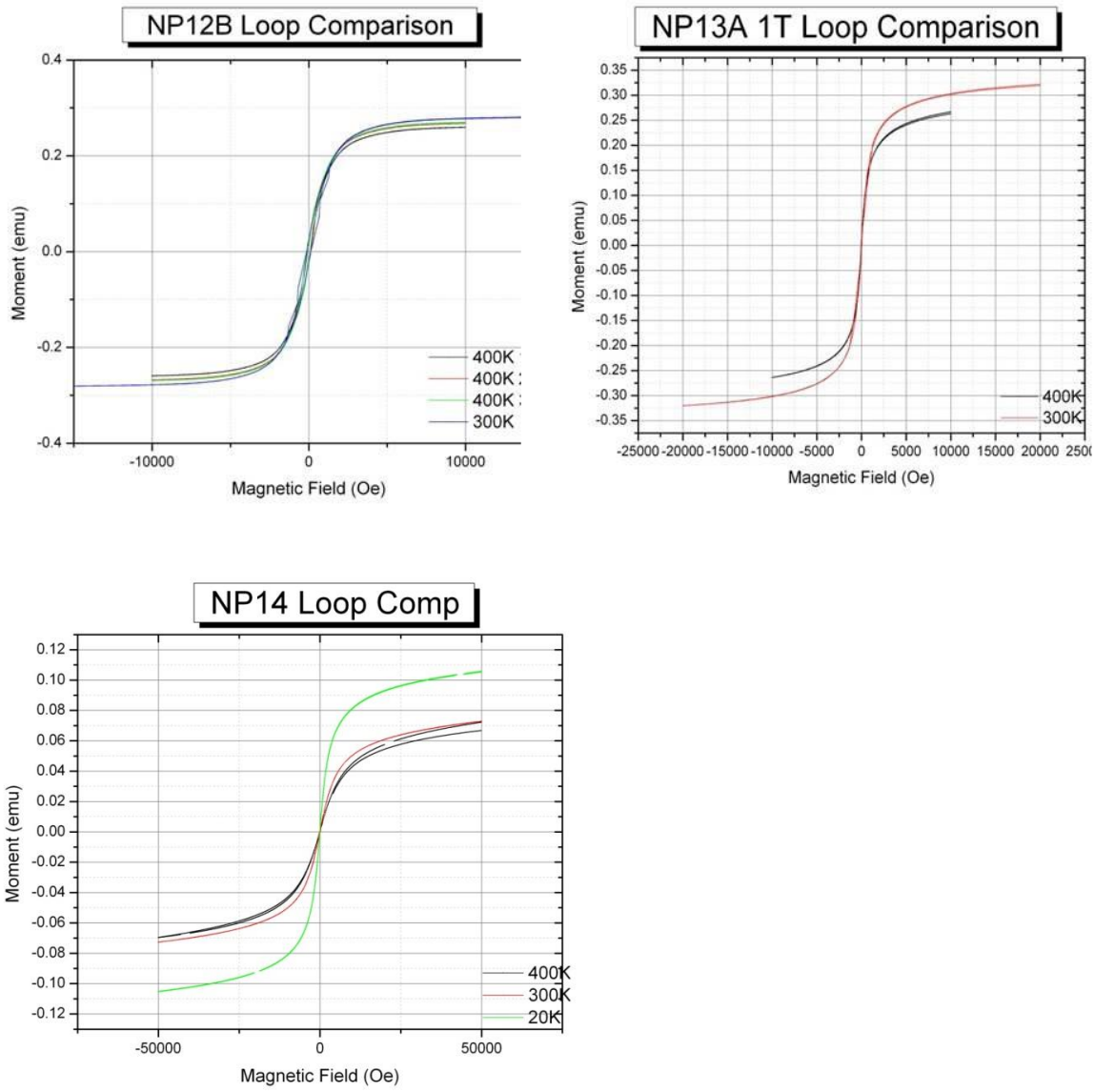

Figure 12 Magnetic loops measured at various temperatures for the three types of samples: Inorganic Salt (NP12B), Inorganic Solution (13A), and Organic Solution (NP14) respectively

We have studied if there is a change in the saturation point when the temperature changes, as seen in figure 12. We do not see much of a change as to where the saturation field H_S is, but we do see a change in the slope around the origin and also a change in the amount of magnetic moment at saturation, M_S. For we see that the lower the temperature, the higher the slope at zero and the higher magnetic moment at saturation M_S.

We have also studied if the loops have any sign of a hysteresis. Hysteresis means that on the way up and down and back up the points are not the exact same, meaning that they do not cross the same path twice. We do this by zooming in around the zero point on both the x- and y-axis, as seen in figure 13. We then can see how wide the hysteresis is. The wider it is the harder it is for the particles to follow the same path, meaning that the particles are larger in size. The end result is that for smaller particles, we should be seeing a smaller hysteresis loop. This is seen with the results of the examination of the loops. We have noticed that the width of the magnetic loop is around 200 Oe for the inorganic salt method, around 50 Oe for the inorganic solution method, and around 6 Oe for the organic solution method, which is almost insignificant. We conclude that the smaller the particles, the smaller the hysteresis. Even the hysteresis will disappear when the particles are small enough.

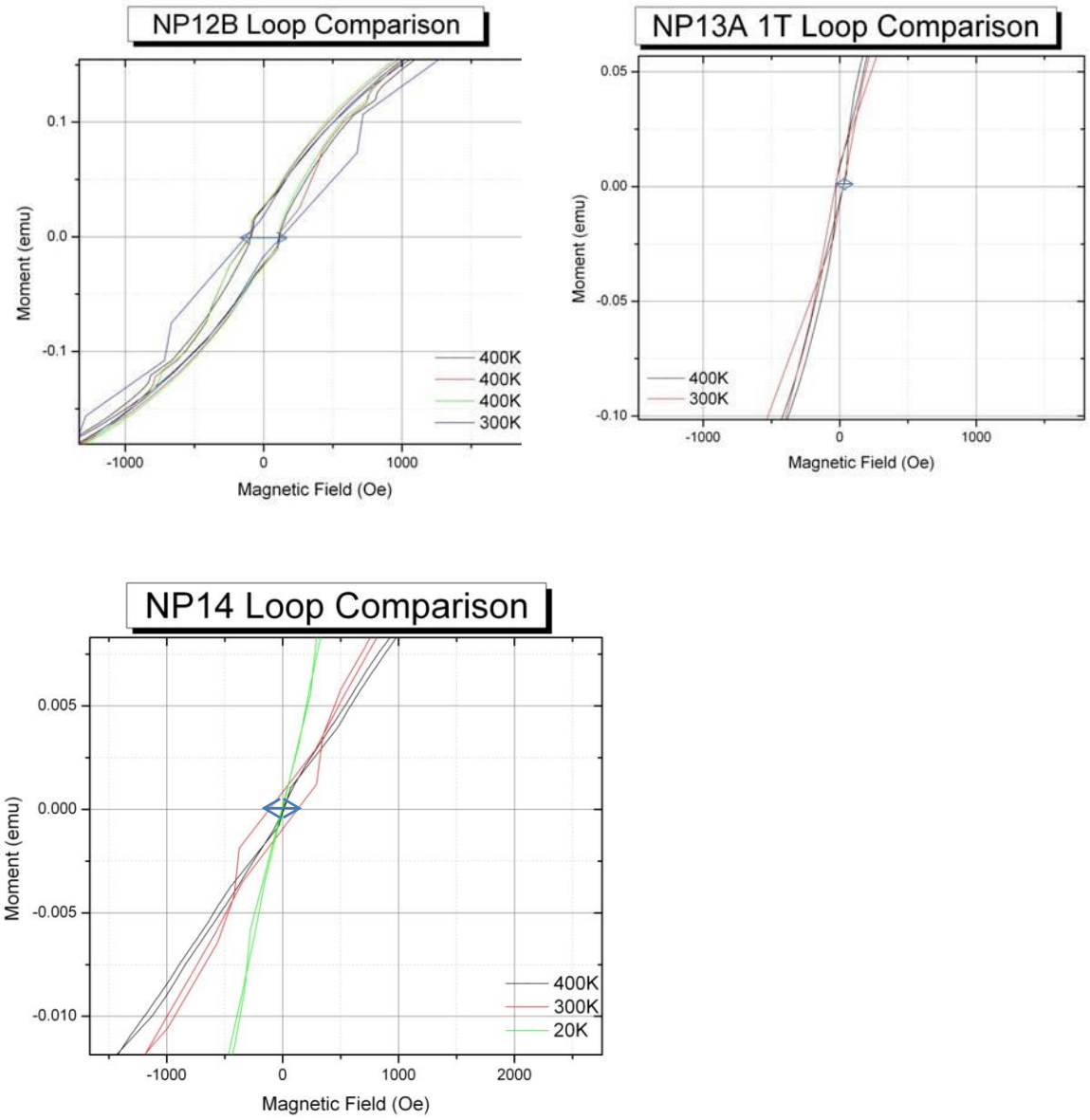

Figure 13 Zoom of Loops from figure 12, width is about 200 Oe Inorganic Salt, about 50 Oe Inorganic Solution, and about 6 Oe Organic Solution, respectively

4.3 Zero Field Cooling and Field Cooling Measurements

After we have established the basic characteristics of the sample, we perform other measurements on the sample. We usually start with a zero field cooling (ZFC). For the ZFC measurement, we usually cooled the sample down from 400K (673 °C) to around 20 K (293 °C) under no magnetic field. We then heated the sample back up under a magnetic field of desired value, and the magnetic moment is measured during the heating process. The ZFC is complemented with a field cooling measurement (FC). For the FC measurement, we cooled the sample down from 400 K to around 20 K and heated back to 400 K, all under the same magnetic field that the ZFC was done at. We then compared the ZFC and the heating part of the FC measurement. At low temperatures, the curves are usually separated, and then join at higher temperature. We associate the blocking temperature to the point where the FC and ZFC curves join. Sometimes the joining point is not as clear and the blocking temperature can be seen by a bump in the ZFC graph. We expect that the larger the particles the higher the blocking temperature will be. What we have noticed is that when we apply higher magnetic fields, above 500 Oe , the blocking temperature is really hard to read, as seen in figures 14-19. We have more recently started to look at the ZFC and FC measurements under lower magnetic fields, as seen in figure 20. This has allowed us to see the blocking temperature much better. We now need to collect data on all of the samples in order to make a more accurate conclusion on the blocking temperature. Table 5 gives an indication of our estimation of the blocking temperature for the various samples. The estimate is quite accurate for the latest measurements done on sample NP17.

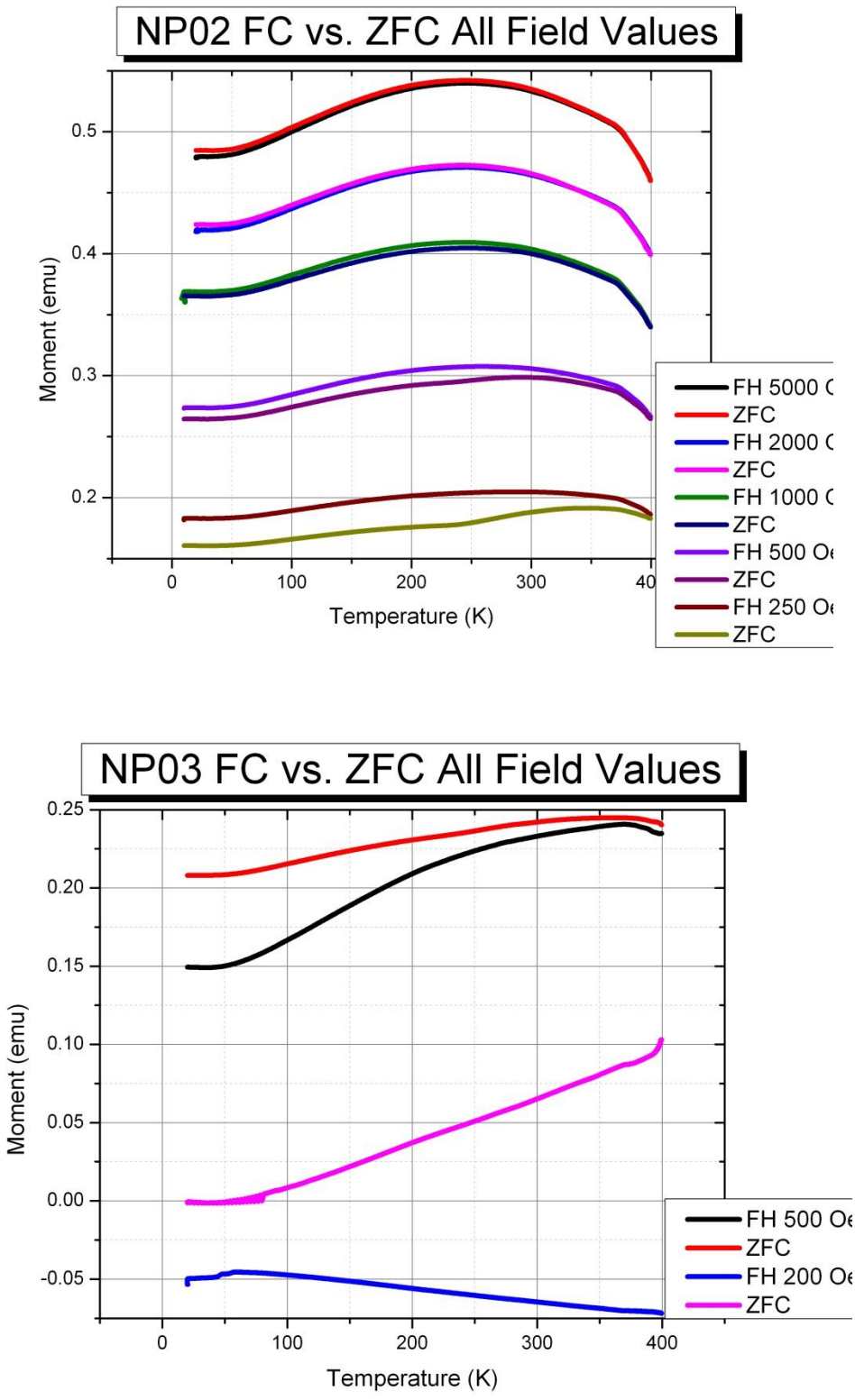

Figure 14 FC vs. ZFC graphs for NP02 and NP03

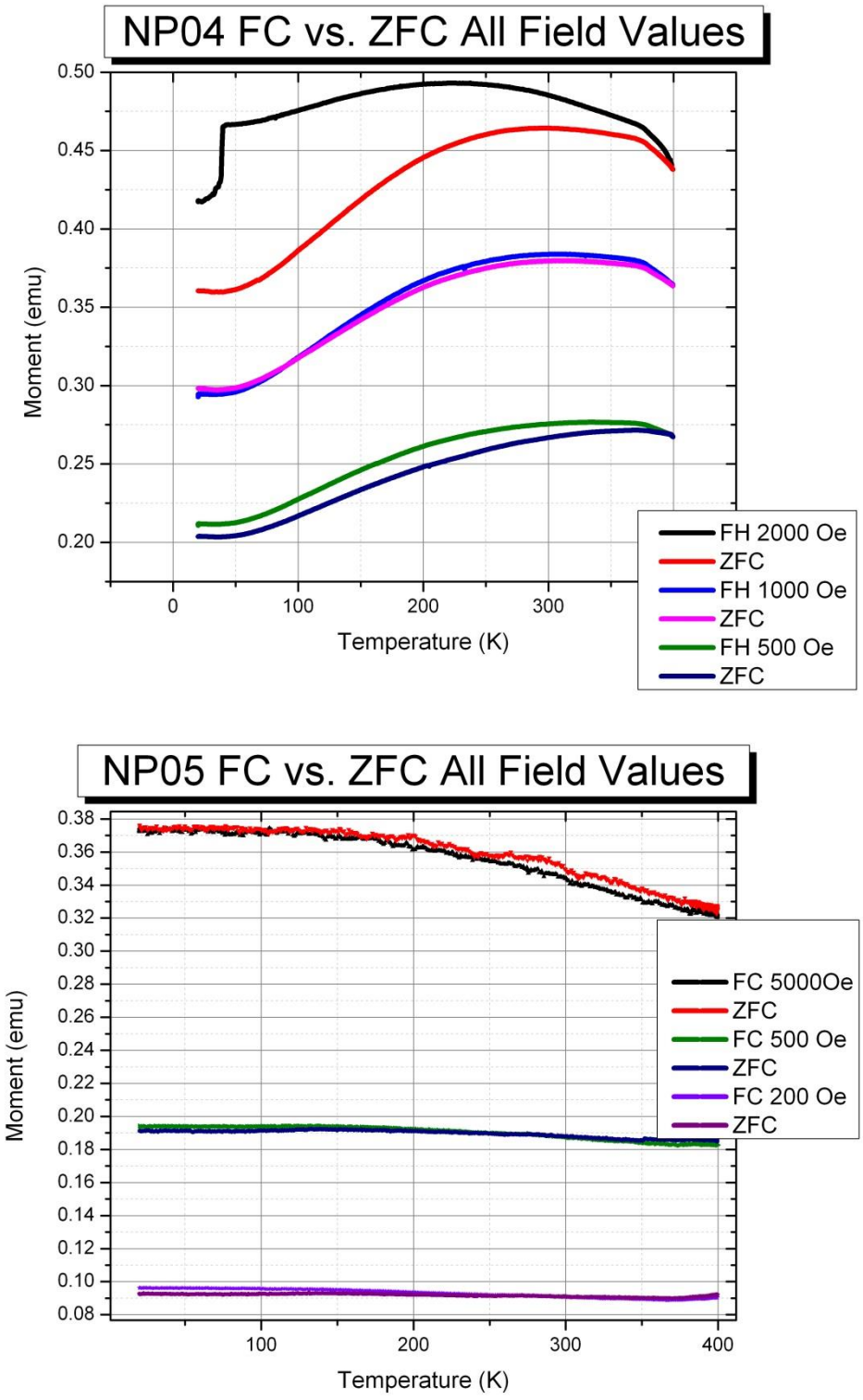

Figure 15 FC vs. ZFC graphs for NP04 and NP05

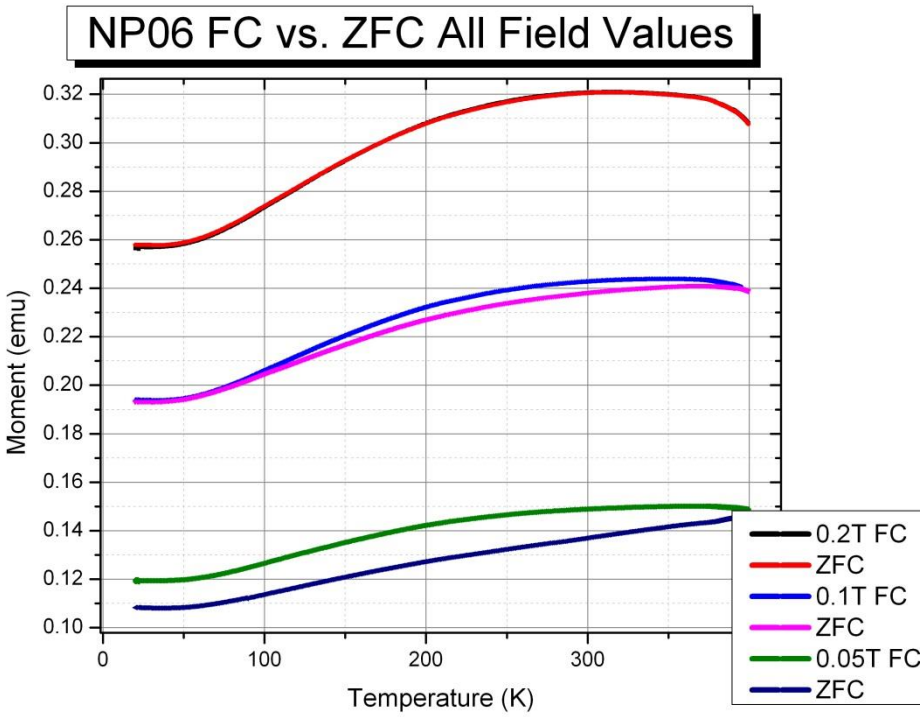

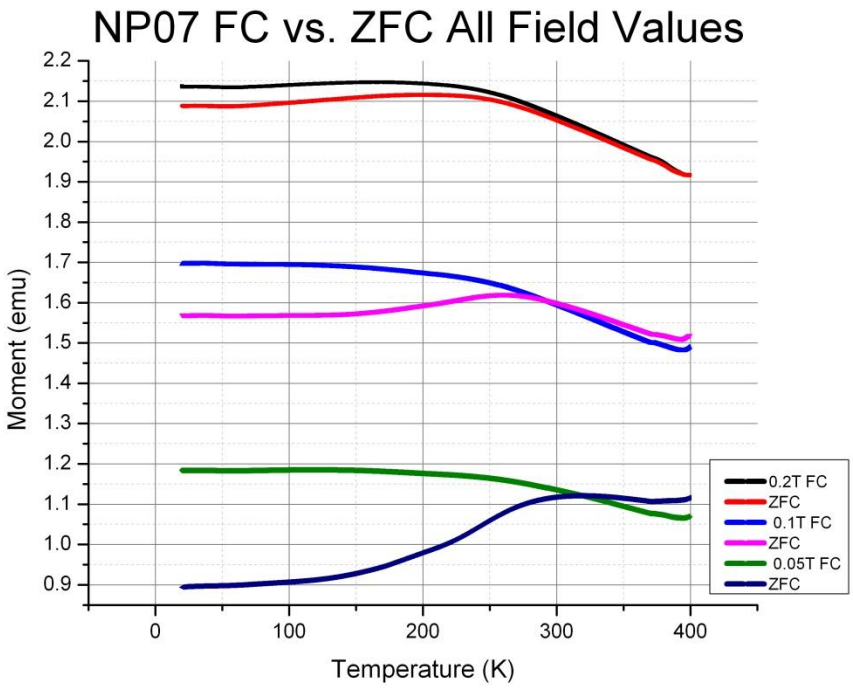

Figure 16 FC vs. ZFC graphs for NP06 and NP07

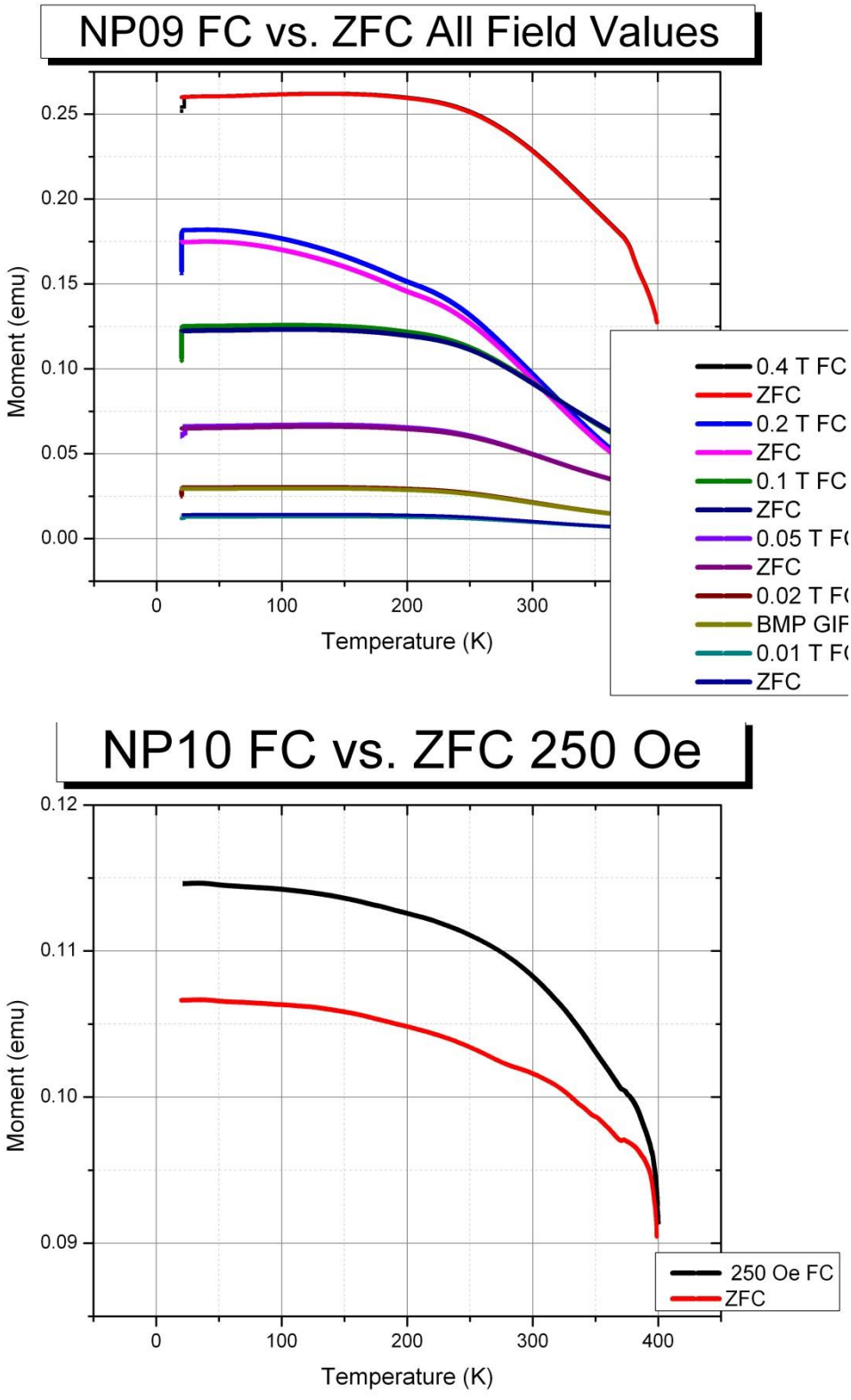

Figure 17 FC vs. ZFC graphs for NP09 and NP10

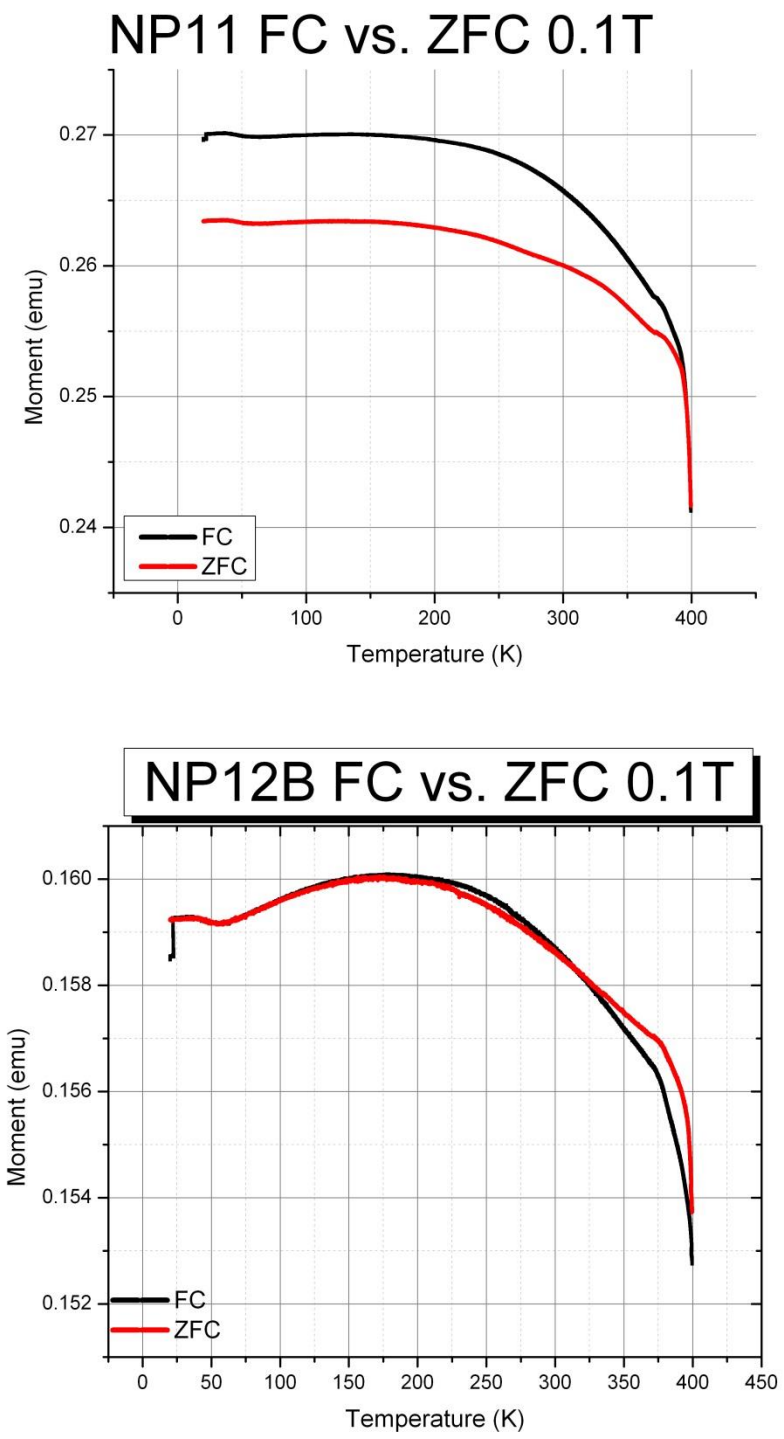

Figure 18 FC vs. ZFC graphs for NP11 and NP12B

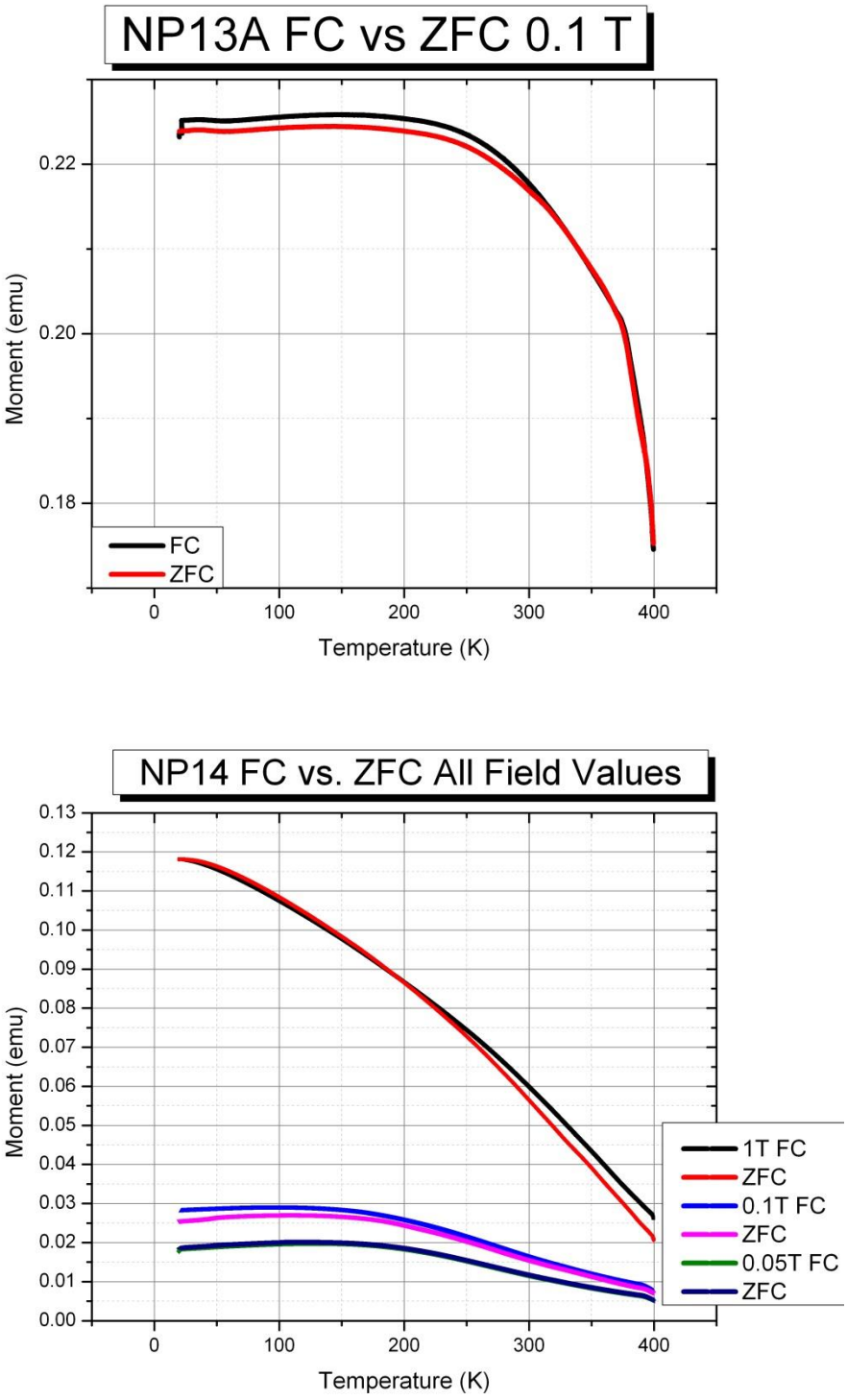

Figure 19 FC vs. ZFC graphs for NP13A and NP14

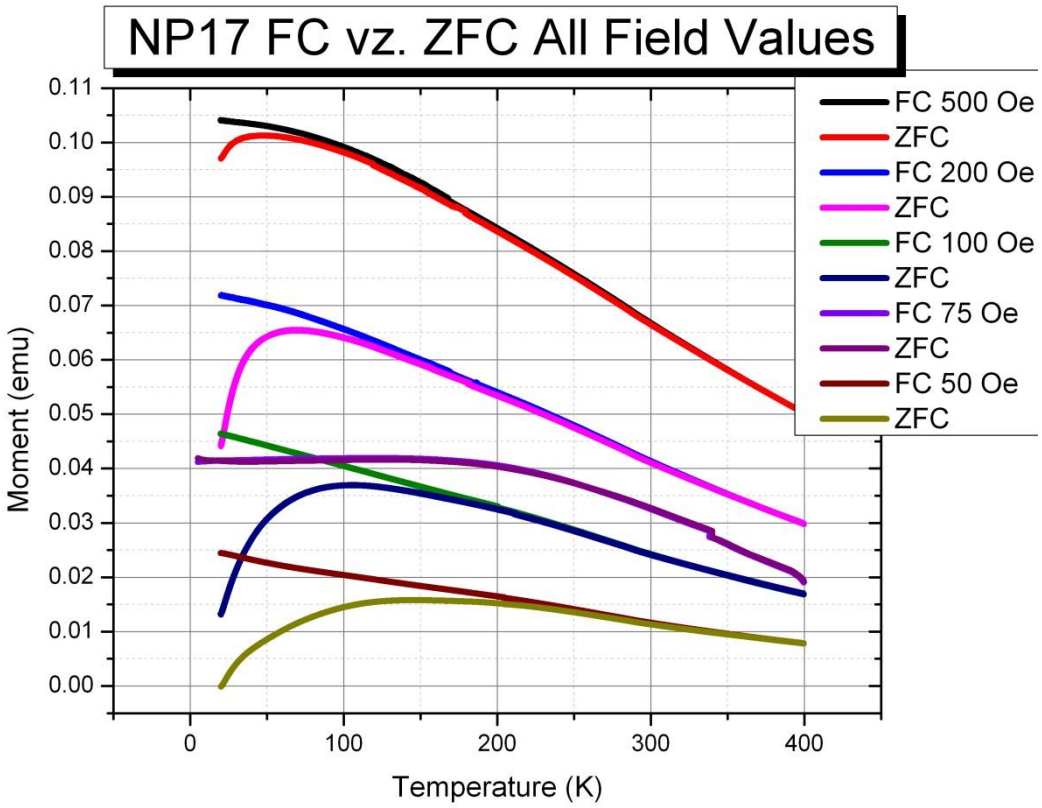

Figure 20 FC vs. ZFC graphs for NP17, Shows there is a definite bump to determine the blocking temperature from

Sample Name	Fabrication Method	Estimate for the Blocking Temperature
NP02	Inorganic Solution	Above 350 K
NP03	Inorganic Solution	Undetermined
NP04	Inorganic Solution	Undetermined
NP05	Inorganic Salt	Undetermined
NP06	Inorganic Slat	Undetermined
NP07	Inorganic Solution	Around 300 K
NP09	Organic Salt	Around 250 K
NP10	Inorganic Salt	Undetermined
NP11	Inorganic Salt	Undetermined
NP12B	Inorganic Salt	Undetermined
NP13A	Inorganic Solution	Undetermined
NP14	Organic Solution	Around 200K
NP17	Organic Solution	Around 100 K

Table 5 Compilation of estimated blocking temperatures for most samples

Chapter 5

Conclusion

We have learned how to fabricate magnetite nanoparticles using different methods; an inorganic salt, an inorganic solution, and an organic solution method. Each method was rather successful in producing magnetite nanoparticles. We have, however, observed, from XRD and TEM characterizations, that the average size of the produced nanoparticles varies significantly depending on the method used. The inorganic salt method produces the largest size distribution of nanoparticles while the organic solution is the smallest size of nanoparticles with a small distribution of size. We have been able to determine the nanoparticles' size through XRD and TEM, and be able to make sure that we actually made magnetite by using XRD. XRD provides us information about the crystallographic structure of the sample, while TEM gives us a view of the nanoparticles in real space. We have determined that TEM is more accurate than XRD in determining the average size of the particles.

With the magnetization loops, we have learned that there is little to no hysteresis with the nanoparticles. There is also little change in the saturation point when the temperature changes, but the magnetic moment increases when the temperature of the sample decreases. This gives us an idea for the ZFC and FC measurements. We have been doing these measurements with a high magnetic field and have found that it is hard to determine the blocking temperature of the sample, when an applied magnetic field is too high. We have then started to do the ZFC and FC measurements with lower magnetic field values. This has

facilitated the reading of the blocking temperature. This will hopefully show us that the bigger the particle, or size distribution, the lower the blocking temperature is.

Bibliography

[1] Majewski, Peter and Thierry, Benjamin, Functionalized Magnetite Nanoparticles-Synthesis, Properties, and Bio-Applications, *Critical Reviews in Solid State and Materials Sciences*, 32(3-4), 203-215 (2007)

[2] Goya, G. F., Berquó, T. S., and Fonseca, F. C, Static and dynamic magnetic properties of spherical magnetite nanoparticles, *Journal of Applied Physics*, 94(5), 3520-3528 (2003).

[3] Krycka, K. L., Brochers, J. A., Booth, R. A., Hogg, C. R., Ijiri, Y., Chen, W. C., . . ., Majetich, S. A, Internal magnetic structure of magnetite nanoparticles at low temperature, *Journal of Applied Physics*, 107(9), B525-1—3 (2010).

[4] Krycka, K. L., Both, R. A., Hogg, C. R., Ijiri, Y., Borchers, J. A., Chen, W. C., . . ., Majetich, S. A, Core-shell magnetic morphology of structurally uniform magnetite nanoparticles, *Physical Review Letters*, 104, 207203-1—4 (2010).

[5] Dutta, P., Pal, S., Seehra, M. S., Shah, N., & Huffman, G. P, Size dependence of magnetic parameters and surface disorder in magnetite nanoparticles, *Journal of Applied Physics*, 105(7), B501-1—3 (2009).

[6] Jing, Y., Sohn, H., Kline, T., Victora, R., & Wang, J, Experimental and theoretical investigation of cubic FeCo nanoparticles for magnetic hyperthermia, *Journal of Applied Physics*, 105(7), B305-1—3 (2009).

[7] Nunes, J. S., de Vasconcelos, C. L., Dantas, T. N. C., Pereira, M. R., & Fonesca, J. L. C, Preparation of acrylic latexes with dispersed magnetite nanoparticles, *Journal of Dispersion Science and Technology*, 29, 769-774 (2008).

[8] Woodfield, B. F., Liu, S., Boerio-Goates, J., Liu, Q, Preparation of uniform nanoparticles of ultra-high purity metal oxides, mixed metal oxides, metals, and metal alloys, WO2007098111A2 (2007).

[9] Qingyuan Liu, Preparation of Fe3O4 Magnetic Fluid with Polyether Carrier, Master's Thesis, Beijing Institute of Technology, (1996).

[10] Altavilla, Claudia, Ciliberto, Enrico, Gatteschi, Dante, and Sangregorio, Claudio, A New Route to Fabricate Monolayers of Magnetite Nanoparticles on Silicon, *Advanced Materials*, 17, No. 8 (2005).

[11] Jana, Nikhil R., Chen, Yongfen, and Peng, Xiaogang, Size- and Shape-Controlled Magnetic (Cr, Mn, Fe, Co, Ni) Oxide Nanocrystals via a Simple and General Approach, *Chemistry of Materials*, 16, 3931-3935 (2004).

[12] Park, Jongnam, An, Kwangjin, Hwang, Yosun, Park, Je-Geun, Noh, Han-Jin, . . ., Hyeon, Taechwan, Ultra-large-scale syntheses of monodisperse nanocrystals, *Nature Materials*, 3, 891-895 (2004).